https://dx.doi.org/10.21577/0103-5053.20230079

J. Braz. Chem. Soc., Vol. 34, No. 12, 1863-1876, 2023

Article

Model Membranes and Antimicrobial Activities of pH-Sensitive Copolymers

Greice K. Saraiva,[a] Valdomiro V. de Souza,[a] Luciana C. de Oliveira,[a] Alyne Procópio,[a] Maisa T. Martins,[a] Isabel N. Aidar,[a] Ronaldo C. F. Yi,[a] Caroline D. Lacerda,[a] Gustavo P. B. Carretero,[a] Rafael B. de Lira,[a] Karin A. Riske,[b] Roberto K. Salinas,[a] Hernan Chaimovich,[a] Fábio H. Florenzano[c] and Iolanda M. Cuccovia[,a]*

[a]*Departamento de Bioquímica, Instituto de Química, Universidade de São Paulo, 05508-000 São Paulo-SP, Brazil*

[b]*Departamento de Biofísica, Universidade Federal de São Paulo, 04039-032 São Paulo-SP, Brazil*

[c]*Departmento de Engenharia de Materiais, Escola de Engenharia de Lorena, Universidade de São Paulo, 2602-810 Lorena-SP, Brazil*

Polymers are options as antimicrobials for skin protection, antifouling surfaces, and fabrics. Here we analyzed the interaction of polymers based on poly(methacrylate) (PMMA) and poly((dimethylamino ethyl) methacrylate) (PDMAEMA) with model membranes and bacteria. We used the homopolymers PMMA, PDMAEMA, and the diblock copolymer(s) prepared with different $PMMA_m$:$PDMAEMA_n$ ratios (m/n). The interactions of PDMAEMA and $PMMA_m$-*b*-$PDMAEMA_n$ with large unilamellar vesicles (LUVs) prepared with phosphatidylcholine and phosphatidylglycerol at different pHs, were analyzed by nuclear magnetic resonance (NMR), dynamic light scattering, and zeta potential. These polymers promoted LUVs leakage of a fluorescent probe (5,6-carboxyfluorescein) localized exclusively in the internal aqueous compartment. Interestingly, all copolymers exhibit a bell-shaped pH dependence for the polymer-induced LUVs leakage. The interaction of the positively charged polymers and the pH effect was also demonstrated using giant unilamellar vesicles. These copolymers inhibited bacterial growth in the micromolar range and can be used to prevent bacterial growth on surfaces.

Keywords: block copolymers, pH-sensitive polymers, antimicrobial polymers, model membranes, membrane binding polymers, copolymer-induced vesicle leakage

Introduction

Antimicrobial polymeric materials (APMs) are options to prepare antifouling surfaces, antimicrobial fabrics, and decontamination systems.[1,2] As polymeric materials can be immobilized on surfaces or particles, their antimicrobial properties only depend on cell membrane interactions, with no internalization. Depending on the application, these properties, and low mammalian toxicity, make polymers more functional than small molecules such as antibiotics.[3,4]

The most common APMs consist of cationic polymers with permanent or pH-dependent charges.[5] The antibacterial activity of APMs depends on coulombic interactions with the negatively charged membranes of Gram-negative and Gram-positive bacteria.[6] Negatively charged phospholipids in the cell wall of Gram-positive bacteria, such as teichoic and lipoteichoic acids, and many others negatively charged on the outer membrane of Gram-negative bacteria, are the primary targets for such interactions.[7] Liposomes bearing negatively charged lipids have proven a valuable model to study interactions that play a fundamental role in the antibacterial effects. In negatively charged liposomes, following initial electrostatic interactions, a hydrophobic-dependent membrane penetration of the antimicrobial agent occurs.[8]

APMs bound to the bacterial surface change cell permeability and produce inner K^+ loss and bacteriostasis.[5-7] Fungi and enveloped viruses are also susceptible to cationic polymers by mechanisms that depend on coulombic interactions at the cell surface.[9] Metal chelation and hydrophobic interactions have also been invoked to play roles in the antimicrobial effects of polymers, mainly when the coulombic result is weak.[10]

*e-mail: imcuccov@iq.usp.br
Editor handled this article: Fernando C. Giacomelli (Associate)

Many factors are related to the polymer's capacity to kill bacteria and other microbes: the polymer or copolymer nature (that reflects on properties like charge density and hydrophilicity)[11,12] and molecular weight.[13] Such parameters may also be essential to the material toxicity towards mammalian cells. For instance, the hydrophilic/hydrophobic balance is crucial in mammalian toxicity related to APMs.[14] Tailoring these and other parameters constitutes a road to better antimicrobial polymers, yielding higher efficiency to kill or inhibit microbes' growth and low human toxicity.[15]

Reversible Deactivation Radical Polymerization (RDRP) comprises many synthetic techniques that control the polymer characteristics, including some crucial for obtaining efficient antimicrobial material.[16] Reversible Addition-Fragmentation Chain Transfer Polymerization (RAFT) generates polymers with characteristics planned from many monomers.[17,18] As molecular weights, chain shapes, and composition of polymers can be tailored, RAFT has been used to obtain APMs.[19,20] All the polymeric materials used in this work were synthesized using RAFT.

Here, poly((dimethylamino ethyl) methacrylate), PDMAEMA, and poly(methyl methacrylate), PMMA, as well as the block copolymers (PMMA-*b*-PDMAEMA) (Scheme 1), were studied to verify their ability to bind to large unilamellar vesicles (LUVs) prepared with phosphatidylcholine (PC) and 1-palmitoyl-2-oleoyl-*sn*-glycero-3-phospho-(1-rac-glycerol), PG, at different molar ratios (PG:PC). Adding a hydrophobic PMMA chain to the PDMAEMA block opened another possibility of interaction with the vesicles, possibly increasing its binding through the insertion of the hydrophobic part of the polymer in the bilayer interface, improving the leakage efficiency, as well as its microbicidal effectiveness against microorganisms.

This work aimed to understand how the interaction of the polymeric materials with the lipid surfaces depends on the charge of the LUVs prepared with different PC:PG ratios and polymer properties such as the hydrophilic/hydrophobic balance and average molar mass.[21] The values of the pK_a of the amino group of DMAEMA are in the 8.4 to 8.6 range[22,23] but, in the polymer, the ammonium groups dissociate[24] between pH 6 and 8 due to the interplay of the groups in the chain, as described for confined polymers of PDMAEMA.[22]

The interaction of the different polymers with the LUVs was studied following the leakage of fluorescent probe 5,6-carboxyfluoresceine, CF, incorporated in the aqueous compartment of the vesicles and by measuring the change in the LUVs charge and aggregation. This interaction was also studied by nuclear magnetic resonance (NMR) spectroscopy, and its effectivity, and pH dependence, on the vesicle, or bilayer, was directly visualized in giant vesicles using optical microscopy.

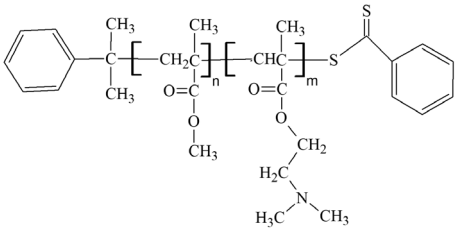

Scheme 1. General structure of the copolymers $PMMA_m$-*b*-$PDMAEMA_n$. All copolymers start with a cumyl and end with the dithiobenzoate group due to the synthesis method (RAFT).

Experimental

Materials

Egg phosphatidylcholine, PC, was extracted from egg yolk and purified as described.[25] The sodium salt of 1-palmitoyl-2-oleoyl-*sn*-glycero-3-phospho-(1-*rac*-glycerol), PG, was obtained from Avanti polar lipids (Alabaster, AL, USA). Sephadex G-25 medium, dichloromethane, methanol, hydrofluoric acid solution (40%), hydrochloric acid (37%), polydocanol, 2-amino-2-(hydroxymethyl)propane-1,3-diol (Tris), 2-(*N*-morpholino) ethanesulfonic acid (MES), 4-(2-hydroxyethyl)-1-piperazine ethanesulfonic acid (HEPES), *N*-cyclohexyl-3-aminopropanesulfonic acid (CAPS) and boric acid were from Sigma-Aldrich (St. Louis, Mo, USA). Polyvinyl alcohol (PVA), with a molar mass of 45,000 Da, was from Merck Co (Darmstadt, Germany). Polycarbonate membranes (100 nm pore diameter) (Nucleopore, Track-Etch Membrane filters) used for vesicle preparation by extrusion were from Whatman-GE Healthcare (Waukesha, WI, USA).

5(6)-Carboxyfluorescein (CF) from Sigma-Aldrich (St. Louis, USA) was purified as described.[26,27] The solution of the sodium salt of CF was lyophilized and maintained at 8 ºC until use.

Fluorescence measurements were performed in a Hitachi F-7000, Tokyo, Japan, spectrofluorometer in a quartz cell of 2.5 mL, 1 cm optical path. The absorption measurements were done in a Hitachi U 2000 spectrophotometer (Tokyo, Japan). The hydrodynamic diameter, the electrophoretic mobility, and zeta potential were measured in a Zetasizer Nano 317 apparatus (Worcestershire, UK).

Polymers and copolymers

$PMMA_{50}$, $PDMAEMA_{265}$, and copolymers $PMMA_{94}$-*b*-$PDMAEMA_{88}$, $PMMA_{50}$-*b*-$PDMAEMA_{269}$,

and $PMMA_{48}$-*b*-$PDMAEMA_{324}$ (Scheme 1) were synthesized via RAFT as described previously.[28] Briefly, the copolymers were obtained via a two-steps RAFT procedure: the PMMA blocks were synthesized first, using cumyl dithibenzoate (CDB) as the chain transfer agent (CTA), benzoyl peroxide (BPO) as initiator and methyl methacrylate passed through an alumina column for inhibitor removal. The CDB/BPO ratio was three or above in all cases, and the reaction temperature was from 70 to 80 °C. Typically, roughly 50% conversion was reached. The homopolymer was then purified by precipitation in methanol after solubilization in tetrahydrofuran (THF) (three times) and subsequently used as macroCTA in a batch copolymerization with DMAEMA as monomer and BPO as initiator. Copolymerizations lasted around 24 h. The copolymers were purified by solubilization in THF and precipitation in hexane (three times). In-depth characterization data, including proton NMR and gel permeation chromatography (GPC), can be found in our previous work.[28] Table 1 summarizes the characteristics of the polymers used here. All copolymers start with a cumyl and end with the dithiobenzoate group, which is very small compared with the polymer molecular weight and should not interfere with the main properties of the polymers.

Methods

Phospholipid concentration determination

The phospholipid concentration of the vesicle pool was determined from inorganic phosphate analysis using the method of Rouser *et al.*,[29] adapted by Manzini *et al.*[27]

Polymer solutions

Polymer(s) and copolymer(s) concentrated stock solutions were prepared in methanol. Stock solutions were used to prepare all buffered polymer solutions (< 5% methanol) to avoid solvent interference in the experiments.

Preparation of the large unilamellar vesicles (LUVs) with CF

LUVs were prepared using dichloromethane concentrated stock solutions of PC and PG (9 mg mL^{-1}), mixed at the proportion desired in a test tube. The solvent was eliminated with an N_2 flux, rotating the tube until a thin lipid film was obtained. The tubes were maintained in a desiccator linked to a vacuum pump for 1 h to eliminate residual solvent. A solution of CF 50 mM in 10 mM Tris-HCl buffer, pH 8.1, was added to the lipid film-containing tube, and the tube was vortexed until complete film detachment. This suspension is known to contain multilamellar lipid vesicles, MLVs. Large unilamellar vesicles (LUVs) of similar sizes were obtained by passing the MLVs suspension (×11) through two stacked polycarbonate membranes of 100 nm at room temperature, using a LiposoFast extruder (Avestin Inc., Ottawa, Canada).[30]

For preparing CF-loaded LUVs, the lipid films were hydrated with 0.5 mL of 50 mM CF sodium salt in 10 mM Tris-HCl buffer, pH 8.1, yielding a final lipid concentration of 17 mM. External CF was removed by passing the LUVs (ca. 0.5 mL) through a Sephadex-G 25 column (0.8 × 20 cm), eluted with 10 mM Tris-HCl buffer pH 8.1 and 300 mM NaCl to maintain the osmolarity of the CF solution.[27] The Sephadex-G25 column was previously saturated with sonicated vesicles, with the same lipid composition as the LUVs, and eluted with 10 mM Tris/HCl, pH 8, 300 mM NaCl. LUVs were collected in 2 mL at the void volume, and the pool was maintained in an ice bath until use.

Measurement of the CF leakage from LUVs by fluorescence

The CF fluorescence in the internal aqueous compartment of the vesicles, at the concentration used in these experiments, was quenched. To determine the effect of the copolymers in the CF leakage from the LUVs, an aliquot of 90 µL of CF-containing LUVs was added to the fluorescence cell containing buffer (the final volume in each experiment was 2 mL). The fluorescence was determined at λ_{em} = 520 nm (λ_{exc} = 490 nm) as a function of time. After 100 s, the polymer or copolymer was added to the cuvette under constant stirring using a magnetic bar. The final percentages of methanol, from the polymer solution, in these experiments were all less than 5%. Adding methanol,

Table 1. Characteristics of the polymeric materials used in this work

Polymer	Mn × 10^{-3} / (g mol^{-1})	Mw/Mn	PDMAEMA mass fraction[a]
$PMMA_{50}$-*b*-$PDMAEMA_{269}$	46.5	1.26	0.89
$PMMA_{48}$-*b*-$PDMAEMA_{324}$	56.0	1.19	0.91
$PMMA_{94}$-*b*-$PDMAEMA_{88}$	23.3	1.10	0.60
$PMMA_{50}$	4.98	1.21	0
$PDMAEMA_{265}$	41.6	2.55	1.00

[a]PDMAEMA mass fraction: (average units of PDMAEMA × molecular mass of DMAEMA)/(average units of PMMA × molecular mass of MMA + average units of PDMAEMA × molecular mass of DMAEMA). Mn: number average molar mass; Mw: weight average molar mass. PMMA: poly(methyl methacrylate); PDMAEMA: poly((dimethylamino ethyl) methacrylate).

at this percentage, to the vesicles, without polymer, did not affect the vesicle permeability. Fluorescence was measured, at 25 ºC, for 450 s, then 30 μL of an aqueous solution of polydocanol 10% v/v were added to attain complete permeabilization of the LUVs, obtaining the fluorescence maximum.

The percentage of leakage in each kinetic run was calculated using equation 1:

$$\text{Leakage (\%)} = \frac{(I_t - I_0)}{(I_{tot} - I_0)} \times 100 \quad (1)$$

where I_o was the initial fluorescence intensity before polymer addition, I_t was the fluorescence after polymer addition at time t, and I_{tot} was the total fluorescence after polydocanol addition. All experiments were done in duplicate and the maximum difference between runs was 10%.

Measurement of polymer-induced CF leakage at different pHs

The effect of the protonation of the polymer amino groups on LUVs permeabilization was studied using LUVs containing different PC:PG molar ratios. The LUVs were prepared using 0.5 mL of 50 mM CF in 10 mM Tris/HCl, pH 8. LUVs containing CF were applied into the Sephadex column and eluted with a buffer containing 10 mM Tris/HCl, pH 8, and 300 mM NaCl, as described before. LUVs eluted in the void volume of Sephadex were collected, and the phospholipid concentration of the vesicle pool was determined before use. To study the effect of pH on the kinetics of CF leakage, an aliquot of 90 μL of LUVs containing CF collected in the previous step was added to the cuvette containing 2 mL of 10 mM buffer prepared at different pHs and 300 mM NaCl to maintain the osmolarity. The external pH was changed only when the kinetic assay was performed in the fluorimeter. The fluorescence of CF was determined at λ_{em} = 520 nm (λ_{exc} = 490 nm) as a function of time at 25 ºC. The kinetic assay consisted of an initial 100 s reading of the fluorescence of CF, polymer addition, and its kinetic monitored for 400 s. After that time, 30 μL of 10% (v/v) polydocanol were added to obtain the complete leakage of LUVs, corresponding to 100% CF leakage. The following buffers (10 mM) contained 300 mM NaCl: (*i*) MES pH 6.0; (*ii*) HEPES pH 7.0; (*iii*) HEPES pH 7.5; (*iv*) Tris/HCl pH 8.0; (*v*) Tris/HCl, pH 8.5; (*vi*) borate, pH 9.0; (*vii*) CAPS, pH 10.0.

Determination of hydrodynamic diameter (D_h), electrophoretic mobility (U_E), and zeta potential (ζ)

LUV hydrodynamic diameter (D_h) and electrophoretic mobility were measured in a Zetasizer Nano apparatus with a 633 nm laser (Malvern, Worcestershire, UK). The zeta potential (ζ) is given by equations 2 and 3 applying the Smoluchowski theory, and electrophoretic mobility (U_E) was calculated using Henry's, Smoluchovski approximation (equations 2 and 3).

$$U_E = 2\varepsilon\zeta f(ka)/3\eta \quad (2)$$

$$\zeta = \eta U_E/\varepsilon \quad (3)$$

where U_E: electrophoretic mobility; ζ: zeta potential; ε: dielectric constant; f(ka): Henry function; η: viscosity.

The LUVs D_h, ζ, and U_E were determined at 25 °C in a quartz cuvette. The buffer was previously filtered using a 0.22 μm diameter pore Millipore membrane. The values of D_h and UE were the average of three measurements of the same sample. For D_h and U_E measurements, 20 μL of 25 mM LUVs solution were added to 1 mL of 10 mM Tris/HF pH 8.5 buffer. With a final lipid concentration of 0.5 mM, interparticle interactions are irrelevant since the vesicle concentration is in the nanomolar range.[31] The values of D_h are all number averaged.

After initial measurements of D_h and UE of the LUVs, aliquots of the polymers were added to the samples from a stock solution generally containing 6×10^{-6} M, depending on the polymer, prepared in 10 mM Tris/HF, pH 8.5, buffer. Additional measurements were performed to determine the surface's particle size and electrical potential effects. Volumes ranging from 5 to 200 μL of copolymer solution were added to 1 mL of buffer containing LUVs. The following parameters of the DLS were used: water as a dispersant, refraction index of 1.33, viscosity of 0.792 cP, dielectric constant of 76.8, and 25 ºC.

Giant unilamellar vesicles (GUVs)

For GUVs preparation, 100 μL of 5% (p/v) polyvinyl alcohol (PVA) solution was spread over a glass slide to form a thin film.[32] The glass slide was maintained at 70 ºC for 15 min in an oven. After drying the PVA solution, 10 μL of 2 mg mL^{-1} (2.5 mM) of phospholipids dissolved in $CHCl_3$ were spread over the PVA layer. The residual solvent was removed with a stream of N_2. A Teflon frame was added over the glass slide, and another glass slide was placed over the Teflon frame to form a chamber sealed with paper clips. The chamber was filled with 1 mL of a buffer solution containing 200 mM sucrose and 100 mM NaCl and maintained for 20 min at room temperature. The observation chamber was filled with 80 μL of a copolymer solution with a defined concentration prepared in the same pH of the internal buffer, with 100 mM NaCl, as used to grow the GUVs and containing 200 mM glucose. Different GUVs preparations were done using buffers of various

pHs. In all cases, the pH of the buffers inside and outside was equal. The buffers (10 mM) were: MES, pH 6.0; Tris/HCl, pH 8.5 and CAPS, pH 10.0. Then, 20 µL of GUVs suspension was added to the observation chamber, and the GUVs were observed in an inverted Zeiss Axiovert 200 (Jena, Germany) microscope equipped with phase contrast 20×, 40×, and 63× objectives. Image acquisition with a Zeiss AxioCam HSm digital camera (Jena, Germany) was started immediately.

^{1}H NMR studies of the effect of pH on the structure of $PMMA_{48}$-*b*-$PDMAEMA_{324}$ and its interaction with LUVs of PC:PG 90:10

The interaction of $PMMA_{48}$-*b*-$PDMAEMA_{324}$ with LUVs was analyzed by ^{1}H NMR. The NMR experiments were performed using a Bruker Avance III spectrometer (Billerica, Massachusetts, USA), operating at 500 MHz (^{1}H frequency). NMR samples with a total volume of 0.5 mL were conditioned in a 5 mm NMR tube, and NMR experiments were recorded at 25 ºC. The stock solutions of $PMMA_{48}$-*b*-$PDMAEMA_{324}$ (2 mM) were prepared in methanol-d_4, 99.8%, and the LUVs (PC:PG 90:10) were 2 mM in total lipid prepared in the adequate buffer. The NMR buffers were sodium phosphate 10 mM for the pHs 6.2, 7.0, and 8.1 and sodium borate 10 mM for pH 10, supplemented with 10% (v/v) D_2O. The spectra of $PMMA_{48}$-*b*-$PDMAEMA_{324}$ in $CDCl_3$ were previously acquired, and the ^{1}H assignments were transferred from previously published data.[28] Proton one-dimensional NMR spectra were derived from the 1st increment of nuclear Overhauser effect spectroscopy (NOESY) experiments recorded with 1H 90^o pulses of 8 µs, using water pre-saturation and NOE mixing time of 120 ms. A total of 2048 points were acquired in a spectral window of 6000 Hz, corresponding to a resolution of approximately 3 Hz *per* point. The NMR spectra were processed using Bruker Topspin software and aligned to the residual water line.

Evaluation of antimicrobial activity

Antimicrobial activities of copolymers were evaluated by determining their minimum inhibitory concentrations (MIC)[33] against strains of Gram-negative (*Escherichia coli*) and Gram-positive (*Bacillus subtilis*) bacteria. The bacteria were initially grown on an agar plate. Next, a single colony was picked and inoculated in 5 mL of Mueller-Hinton broth (MHB) and incubated overnight at 37 °C with shaking at 200 rpm. Then the sample was diluted 50 times in MHB and incubated until optical density (OD) 0.4 at 600 nm (10^8 colony forming units (CFU) mL^{-1}). A 1:250 dilution in broth provides the bacteria suspension working solution (10^6CFU mL^{-1}). Stock solutions of the copolymers were prepared in methanol. For the broth microdilution method, 10 µL of each copolymer stock solution and 90 µL of broth were placed in the first well of the line in a 96-well round-bottom microplate, all other wells in the line were filled with 50 µL of broth, and then serial dilutions 1:2 were performed. For each polymer, the experiments with each bacterium were repeated six times. In one line, 10 µL of methanol were added to check the solvent contribution to the antimicrobial activity. Fifty microliters of bacterial suspension were added to each well, yielding a final concentration of approximately 5×10^5 CFU mL^{-1}. A well without an antimicrobial agent containing only bacteria was used as a positive growth control, and only sterile MHB as a negative control. After 18 h of incubation at 37 °C, the MIC was visually determined from the lowest concentration of copolymer at which no bacterial growth was observed. To differentiate whether the copolymer had bactericidal or bacteriostatic activity and to determine the minimum bactericidal concentrations (MBCs), 5 µL of the well in which no bacterial growth was observed was dripped onto a copolymer free agar plate to assess bacterial growth.[34]

Results and Discussion

Leakage of 5(6)-carboxyfluorescein (CF)-containing LUV's induced by PMMA and PDMAEMA

The effect of $PDMAEMA_{265}$ concentrations, [$PDMAEMA_{265}$], on the percentage of CF leakage (CF %Leak) from LUVs with 100% PG, as a function of time, is shown in Figure 1. The baseline of CF %Leak was low and stable for 100 s, indicating that CF did not leak from LUVs spontaneously. After adding $PDMAEMA_{265}$, the fluorescence increased with time, indicating CF leak from the LUVs. The extent of the CF leak strongly depended on polymer concentration (Figure 1A). Polydocanol was added (after 400 s) to obtain 100% of the CF Leak. In Figure1B, the CF %Leak from LUVs of 100% PG, after 200 s, was plotted as a function of [$PDMAEMA_{265}$]. The curve of CF %Leak *vs*. [$PDMAEMA_{265}$] increased non-linearly, showing saturation at about 60% at the highest copolymer concentration. As a LUV of an average diameter of 100 nm (see below) is composed of ca. 10^5 lipid molecules,[31] it was clear that, even with a significant excess of positively charged groups, more than one polymer molecule was necessary to induce vesicle leakage.

CF leakage from LUVs induced by [$PDMAEMA_{265}$] depended on the molar ratio of PC:PG (Figure 1C). As a limit, the polymer did not induce CF leak from LUVs with 100% of zwitterionic PC, and as the PG:PC ratio increased, the increase in polymer activity was evident (Figure 1C). In

Figure 1D, the CF %Leak, after 200 s, obtained from data of Figure 1C, was plotted as a function of the percentage of PG, at [$PDMAEMA_{265}$] of 2.1×10^{-6} M. The CF %Leak increased with the percentage of PG reaching a maximum of 30% with LUVs of 50% PC:PG, decreasing with further increase of the percentage of PG. These results indicate that the copolymer efficiency depends on charge density in the LUVs bilayer under these conditions. However, at 100% PG, a further increase in the CF %Leak was observed.

The positively charged $PDMAEMA_{265}$, when added to negatively charged LUVs, led to CF leakage. The hydrophobic $PMMA_{50}$, at concentrations up to 1×10^{-4} M, under the same conditions used for $PDMAEMA_{265}$ experiments (Figure 1), did not induce CF leak (data not shown). Even if $PMMA_{50}$ interacts with PC-LUVs, this interaction does not modify the bilayer enough to cause LUVs leakage.

To verify if the hydrophobic portion of PMMA linked to the PDMAEMA polymer increased its interaction with the LUVs, we used three copolymers with the following compositions: $PMMA_{94}$-*b*-$PDMAEMA_{88}$, $PMMA_{50}$-*b*-$PDMAEMA_{269}$, and $PMMA_{48}$-*b*-$PDMAEMA_{324}$, Table 1. The synthesis and characterization of these copolymers were described previously.[24]

The effect of $PMMA_{50}$-*b*-$PDMAEMA_{269}$ on CF Leak from LUVs was analyzed by modifying the composition of LUVs and the copolymer concentration (Figure 2).

$PMMA_{50}$-*b*-$PDMAEMA_{269}$ increased the CF %Leak from LUVs with 100% PG. The leakage depended on copolymer concentration (Figure 2A). Figure 2B plots the %Leak of LUVs as a function of copolymer concentrations after 200 s (data from Figure 2A). The CF %Leak depended almost linearly on the copolymer concentration. $PMMA_{50}$-*b*-$PDMAEMA_{269}$ induces CF %Leak of LUVs of different PC:PG molar ratios (Figures 2C and 2D), and a maximum effect was observed at 50% PC:PG. A decrease of the CF %Leak occurred at higher PG percentages, but above 80% PG, the leak percentage increased.

Increasing the percentage of PG in the LUVs also led to a rise in CF %Leak (Figure 2C). From 10 to 20% PG, almost no leak was observed, but as the percentage of PG increased, a maximum of CF %Leak was observed at 50% PG. A decrease of the CF %Leak with a minimum at 80% PG was observed, followed by another increase at 100% PG (Figure 2D). This profile (Figure 2D) was like that with [$PDMAEMA_{265}$], but the decrease of CF %Leak after the peak was not as sharp as that observed with [$PDMAEMA_{265}$].

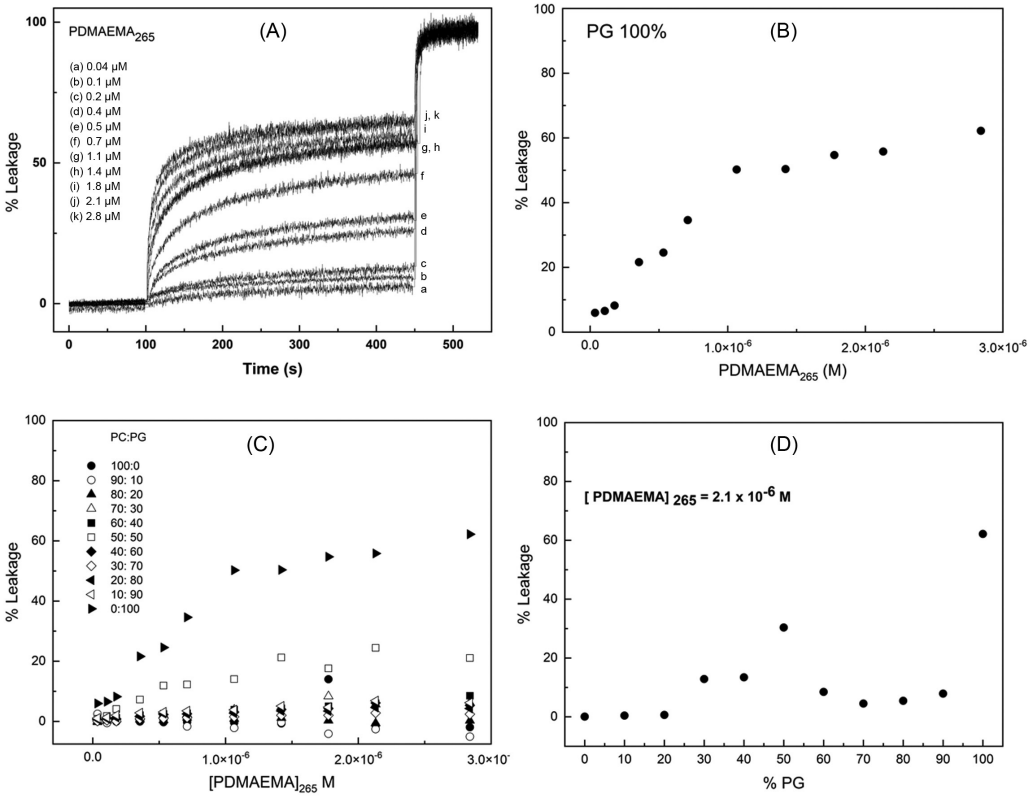

Figure 1. Effect of [$PDMAEMA_{265}$] on CF %Leak of LUVs with different PC:PG molar ratios. (A) Effect of different [$PDMAEMA_{265}$] on CF %Leak of LUVs with 100% PG, as a function of time. (B) Effect of [$PDMAEMA_{265}$] on CF %Leak from LUVs with 100% PG after 200 s. (C) Effect of the [$PDMAEMA_{265}$] on CF %Leak from LUVs with different PC:PG ratios after 200 s. (D) Effect of percentage of PG on CF %Leak of LUVs at [$PDMAEMA_{265}$] = 2.1×10^{-6} M. All experiments were performed in 10 mM Tris/HCl, pH 8.1, 300 mM NaCl buffer. The final concentration of LUVs lipids was 1.44×10^{-4} M.

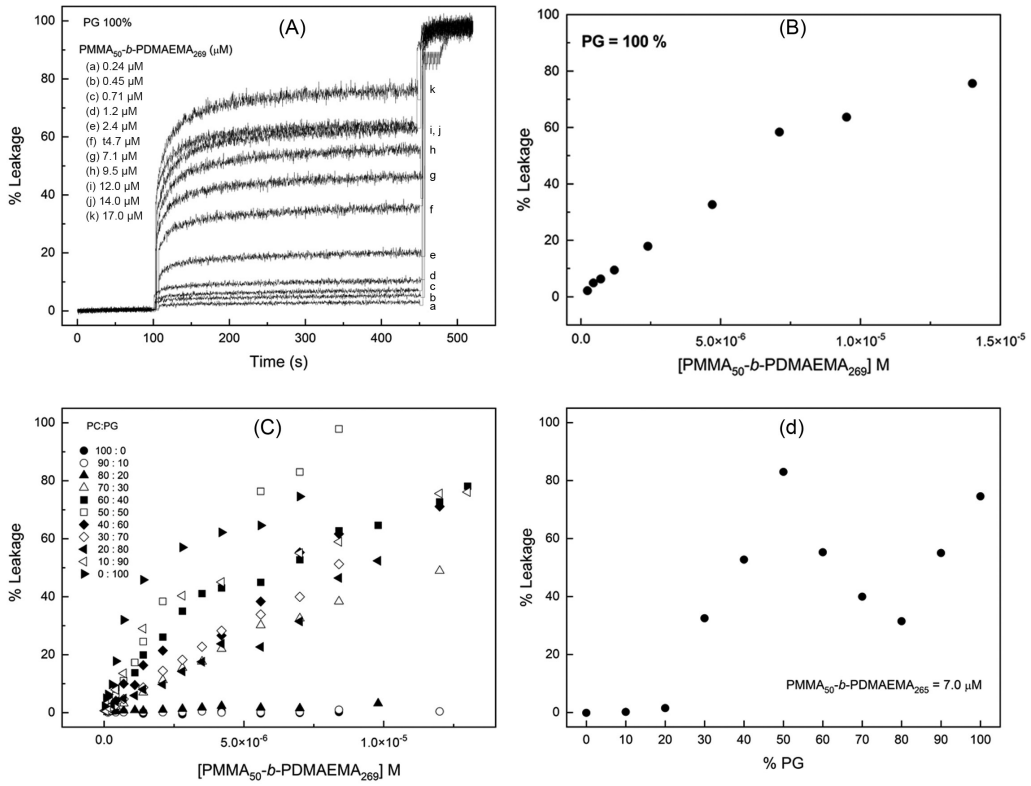

Figure 2. Effect of $PMMA_{50}$-*b*-$PDMAEMA_{269}$ on CF %Leak from LUVs with different PC:PG ratios. (A) Effect of [$PMMA_{50}$-*b*-$PDMAEMA_{269}$] on CF %Leak of LUVs with 100% PG, as a function of time. (B) Effect of [$PMMA_{50}$-*b*-$PDMAEMA_{269}$] on CF %Leak from LUVs with 100% PG after 200 s. (C) Effect of the [$PMMA_{50}$-*b*-$PDMAEMA_{269}$] on CF Leak of LUVs with different PC:PG ratios. (D) Effect of percentage of PG on CF %Leak of LUVs at [$PMMA_{50}$-*b*-$PDMAEMA_{269}$] = 7×10^{-6} M. All experiments were performed in 10 mM Tris/HCl, pH 8.1, 300 mM NaCl, buffer. The final concentration of LUVs lipids was 1.5×10^{-4} M.

The effect of $PMMA_{50}$-*b*-$PDMAEMA_{269}$ on the leakage kinetics profile with PG-LUVs was like that observed with $PDMAEMA_{265}$, but the maximum CF %Leak, as a function of %PG in the LUVs (Figure 2D), was higher, reaching 80% while for [$PDMAEMA_{265}$] the maximum leak at LUVs 50:50 was 40% (Figure 1 D). In Figure 2D, it is also observed that above 80% PG, there is another increase in the CF Leak, indicating that at a high amount of PG, there is no difference between both polymers' efficiency. Increasing the hydrophobicity of the copolymer at moderate PG:PC ratios improved interaction with the bilayer, provoking a more effective destabilization of the LUVs.

With $PMMA_{94}$-*b*-$PDMAEMA_{88}$, where the PMMA:PDMAEMA ratio is close to 1, the decrease in the relative percentage of the positive charge of the copolymer, when compared with $PMMA_{50}$-*b*-$PDMAEMA_{269}$ and $PDMAEMA_{265}$, led to different leak profiles (compare Figures 1, 2, and 3). The differences in the kinetics of the leak profiles and the concentrations producing the maximum CF leak with the three copolymers indicated that the hydrophobic/hydrophilic ratio in their composition led to alterations in the detailed interactions of the polymer with the bilayer.

Effect of pH on the copolymer's leakage of CF from LUVs

The typical pH range where the PDMAEMA amino groups dissociate is between 6 and 8. This extended pH range is due to the dissociation of the amino groups occurring at lower pH than that of the monomeric form.[22] The average ammonium pK_a decreases from 8.4 in the DMAEMA monomer to ca. 7.4 in the polymer (PDMAEMA). This pK_a decrease can be attributed to both charge repulsion by the ammonium units and the local hydroxide concentration near the positively charged copolymer chain.[35] Above pH 9, virtually all the amino groups of the polymers containing $PMAEDMA_{269}$ are dissociated, and the molecule is essentially neutral.

The optimal growth of different microorganisms is pH dependent.[36] The neutrophile microorganisms live at pHs ranging from 5.5 to 8.5, but others can live at extreme pH conditions, such as acidophiles (pH 1 to 6) and alkaliphiles (pH 7.5-11.5). Thus, it is crucial to determine the interaction and efficiency of the polymers as a function of pH, also considering that microorganism growth can change the local pH due to their metabolic activity. To determine the effect of the polymer charge on the disruption of LUVs

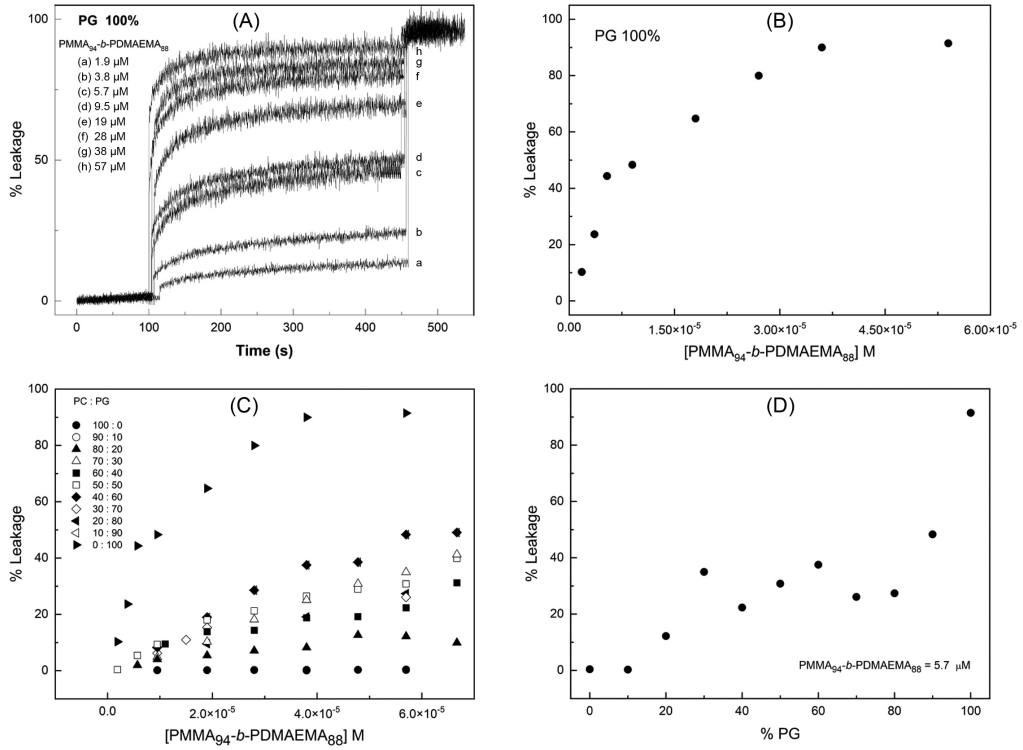

Figure 3. Effect of $PMMA_{94}$-*b*-$PDMAEMA_{88}$ on CF leakage from LUVs with different PC:PG ratios in 10 mM Tris/HCl, pH 8.1, 300 mM NaCl, buffer. (A) Effect of [$PMMA_{94}$-*b*-$PDMAEMA_{88}$] on %Leak of CF of LUVs with 100% PG, as a function of time. (B) Effect of [$PMMA_{94}$-*b*-$PDMAEMA_{88}$] on %Leak of CF from LUVs with 100% PG, after 200 s. (C) Effect of the [$PMMA_{94}$-*b*-$PDMAEMA_{88}$] on CF leak of LUVs with different PC:PG ratios. (D) Effect of percentage of PG on CF leak of LUVs at [$PMMA_{94}$-*b*-$PDMAEMA_{88}$] = 57 μM. In all experiments, the concentration of LUVs lipids was 1.17×10^{-4} M.

with different PC:PG ratios, the CF %Leak from LUVs was studied at several pH's, at fixed polymer concentration (Figure 4). It should be noted that the solubility of CF, as well as the fluorescence,[37,38] decreases below pH 8 due to the protonation of the carboxylate groups. To circumvent this problem, we prepared the LUVs containing CF 50 mM in 10 mM Tris/HCl, pH 8, and the external CF was eliminated through the Sephadex G25 using 10 mM Tris/HCl, pH 8 containing 300 mM NaCl. The kinetics of CF leak of LUVs induced by polymers were determined with different external buffers, all at 10 mM and different pH's, maintaining the ionic strength with 300 mM NaCl. The experiments were initiated by adding the LUV's, with an internal pH of 8.0, to the buffers at different pHs. As the ionic strength of the internal and external buffers was equal, and the kinetics were fast, the pH differences did not affect LUV's stability, demonstrated by the low and stable fluorescence at the beginning of the experiment. The fluorescence only changes after the polymer addition. The final fluorescence was different as a function of the buffer pH. Between pHs 6 and 8, it varies by a factor of two, as demonstrated by Milo *et al.*[38] As the leak percentage of CF is relative to the total solution fluorescence after LUV disruption by the addition of detergent, the absolute values of fluorescence of each experiment are not relevant, and the effect of the pH on the polymer activity can be measured. The CF leakage from LUVs at different external pH, and fixed polymer concentration, was strongly pH dependent (Figure 4).

After 400 s of polymer addition (see Experimental section), the effect of $PDMAEMA_{269}$ on the CF %Leak from LUVs between pHs 6 and 8 was ca. 10% for LUVs with percentage of PG from 10 to 100% (Figure 4a). Above pH 8.0, the CF %Leak increased, reaching a maximum between pH's 8.0 and 9.5, depending on the ratio PC:PG, and decreasing again, to about 10 to 20%, at pH 10.0. The maximum CF %Leak depended on polymer structure, concentration, and the PG:PC ratio of the LUVs. For all polymers, except for PMMA and LUVs of 100% PC, the pH dependency of the CF %Leak was bell-shaped (Figure 4).

Interestingly, for all polymers, the pH effect on leakage was maximum between pH 8.0 and 9.5 and depended on the PC:PG ratio. This pH range coincides with the amino group dissociation region, indicating that the charge is essential to produce LUVs leakage. However, the neutrality of part of the dissociated amino group was fundamental to obtaining a more efficient interaction of the polymers with the bilayer leading to a higher leakage efficiency. The importance of the relationship between polymer charge and hydrophobicity is an essential part of both antimicrobial properties.

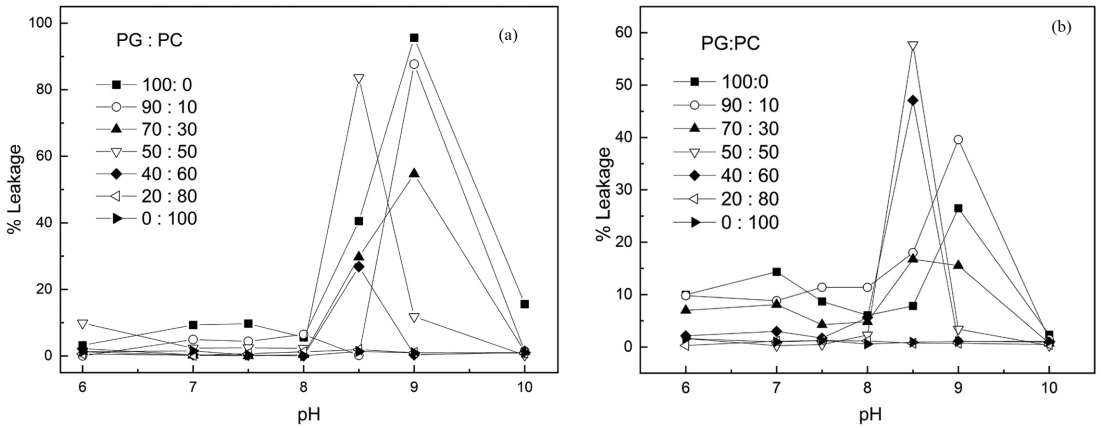

Figure 4. Effect of pH on the CF %Leak from LUVs prepared with different PC:PG ratios at a fixed concentration of (a) $[PDMAEMA]_{269}$ and (b) $PMMA_{94}$-*b*-$PDMAEMA_{90}$. The PC:PG ratios are in the legend inside the figure. The baseline of CF %Leak was followed for 100 s, then the polymer was added, and after 400 s the polydocanol was added to obtain the maximum fluorescence. The concentrations of the polymers were $[PDMAEMA]_{298} = 6.7 \times 10^{-8}$ M and $[PMMA_{94}$-*b*-$PDMAEMA_{98}] = 6.5 \times 10^{-8}$ M, and the concentration of LUV lipids was 1.6×10^{-4} M. The internal buffer of the LUV was 0.01 M Tris-HCl, pH 8.5. As described in the Experimental section, the external buffers contain 300 mM NaCl.

With negatively charged vesicles, the protonated ammonium groups of the copolymers remained attached to the vesicles, and significant leakage occurred. Increasing the pH above 8, part of the ammonium groups dissociates, and the efficiency in the leakage increased to a maximum. Partial ammonium dissociation may lead to further interactions with the bilayer while maintaining the electrostatic component. But the leakage rate decreased significantly when the electrostatic part of the polymer binding to PG-containing LUVs was lost at a higher pH by the full deprotonation of the PDMAEMA ammonium groups. The data in Figure 4 shows that the effect of the polymers on the LUVs leakage is maximum at pH's where the polymer is only partially protonated.

Dynamic light scattering D_h and electrophoretic mobility (U_E)

The effect of polymer-LUVs binding was monitored by measuring the hydrodynamic diameter, D_h, and electrophoretic mobility (U_E) of the LUVs as a function of the polymer concentration in Tris/HF buffer, 0.01M pH 8.5. The effect of $PMMA_{50}$-*b*-$PDMAEMA_{269}$, $PMMA_{48}$-*b*-$PDMAEMA_{324}$, $PMMA_{94}$-*b*-$PDMAEMA_{88}$, and $PMAEDMA_{265}$ on D_h and EM of PC:PG (50:50) LUVs were determined (Figures 5 and S1, Supplementary Information (SI) section). For all copolymers, an increase in the LUVs D_h was observed with a simultaneous decrease in the U_E, indicating aggregation and charge neutralization. Polymer binding to LUVs reduced electrophoretic mobility, dependent not only on the polymer charge but also on the presence of a hydrophobic region of the copolymer. Figure 5 illustrates the behavior for $PMMA_{48}$-*b*-$PDMAEMA_{324}$. The results for all other copolymers are similar, and the figures are in the SI section. For $PMAEDMA_{265}$, the EM of the LUVs increased at polymer concentrations above 2.5×10^{-7} M reaching zero, indicating LUVs binding, while D_h did not vary significantly until that polymer concentration (SI section).

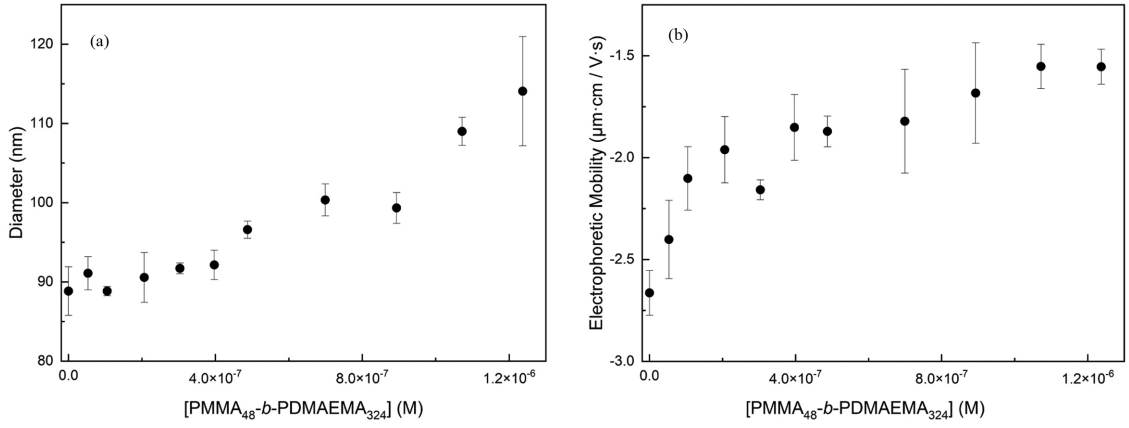

Figure 5. Effect of $PMMA_{48}$-*b*-$PDMAEMA_{324}$ concentration on the diameter (a) and electrophoretic mobility (b) of LUVs of PC:PG (50:50) in Tris/HF buffer, 0.01 M pH 8.5. The concentration of LUVs lipids was 8×10^{-4} M.

Effect of $PMMA_{48}$-*b*-$PDMAEMA_{324}$ on the structure of giant unilamellar vesicles, GUVs, at pH 6.0, 8.5, and 10.0 with 100 mM NaCl

The effect of the polymers on GUVs of PC:PG 50:50 allowed us to obtain information about the mechanisms involved in the permeabilization of the vesicles. The impact of all the polymers on GUVs was observed with vesicles prepared without and with 100 mM NaCl. The buffers in the inner GUV compartment contained 0.2 M sucrose; the external solution was 0.2 M in glucose. The effect of the polymers on GUVs was fast in the absence of salt. Here we only present the results of the copolymer addition on the GUVs prepared with 100 mM NaCl to allow comparison with the data on polymer-induced CF leak (see above). The pH was identical in the inner compartment and external solution in these experiments. The buffers (0.01 M) were MES pH 6.0, Tris/HCl pH 8.5, and CAPS pH 10.0 with 100 mM NaCl. Figure 6 shows representative images of the effect of $PMMA_{48}$-*b*-$PDMAEMA_{324}$ on GUVs of PC:PG 50:50, as a function of time, at different pH's. Initially, the intact GUVs were observed due to the typical optical contrast due to the sucrose/glucose asymmetry across the membrane. Then, the copolymers induced vesicle burst, and this effect was more evident at lower pHs. Figure 6a shows an example of vesicles bursting at pH 6. A pore opens suddenly, and the vesicle collapses, indicating increased membrane tension. Similar patterns were observed for the other copolymers at the same pH (not shown). Figure 6b shows that vesicle collapse occurred at pH 8.5. No effects are observed at pH 10 (Figure 6c) when the copolymer ammonium groups deprotonate, confirming the data of polymer-induced CF leakage. Similar results were obtained with the other copolymers (data not shown).

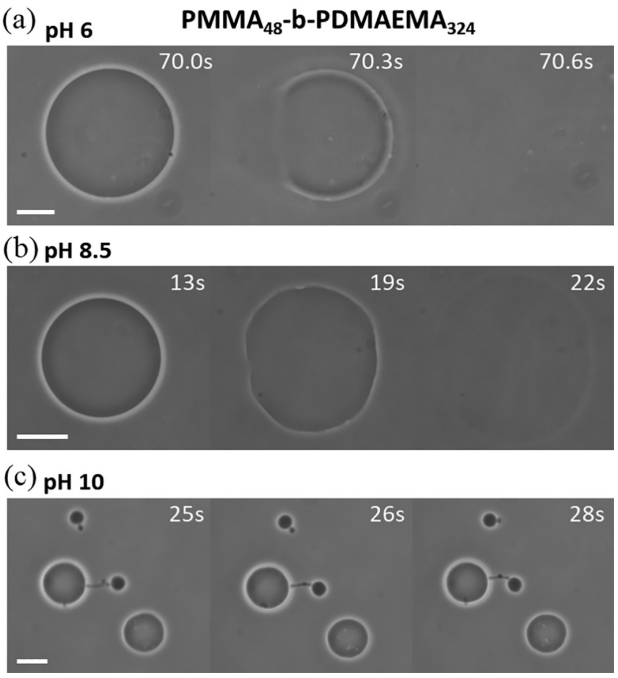

Figure 6. Effect of 5.4×10^{-9} M $PMMA_{48}$-*b*-$PDMAEMA_{324}$ on GUVs composed of PC:PG 50:50 in (a) 0.01 M MES pH 6.0, 100 mM NaCl; (b) 0.01 M Tris/HCl, pH 8.5, 100 mM NaCl; (c) CAPS 0.01 M, pH 10.0 buffer, 100 mM NaCl. Internal and external pH's are the same. The inner GUV solution contains 0.2 M sucrose and the outer solution 0.2 M glucose. The scale bars represent 10 μm.

NMR studies of the interaction of the copolymer $PMMA_{48}$-*b*-$PDMAEMA_{324}$ with PC:PG vesicles (LUVs)

The ^{1}H NMR spectra of the copolymer $PMMA_{48}$-*b*-$PDMAEMA_{324}$ and LUVs of PC:PG 50:50-were obtained in 10 mM phosphate buffer, pH 8.2 (Figure 7). The spectrum of PC:PG LUVs was consistent with the literature,[39] and presented peaks in the range from 0.6 to 1.2 ppm and from 3.1 to 3.5 ppm (Figure 7). The spectrum of the copolymer shows peaks at 2.1 and 2.5 corresponding to the hydrogens of the dimethyl-ammonium group (labeled "a" and "b", respectively) and a peak at 3.8 ppm (labeled "d") corresponding to CH2-O within the side chain of PDMAEMA.[19] Those peaks are well isolated compared to the NMR signals from PC:PG LUVs and were used as reporters to inspect changes induced on the $PMMA_{48}$-*b*-$PDMAEMA_{324}$ spectrum upon adding PC:PG LUVs.

The addition of LUVs to $PMMA_{48}$-*b*-$PDMAEMA_{324}$ induced significant changes in the positions and intensities of the DMAEMA dimethyl-ammonium and CH2-O NMR signals (Figure 7 labeled "a", "b", and "d"). The peaks from the copolymers were slightly shifted ca. 0.05 ppm downfield upon the presence of LUVs. Their line width significantly broadened, as indicated by the decrease in the overall peak intensity (Figure 7, bottom). The chemical shift changes and line broadening were consistent LUVs-copolymer interactions.

The effect of the concentration of LUVs of PC:PG 90:10 on $PMMA_{48}$-*b*-$PDMAEMA_{324}$ at pH 8.2 was investigated by comparing the 1D ^{1}H NMR spectrum of the copolymer at 5.8 mg mL^{-1} recorded in the presence of two different LUVs concentrations: 2 and 6 mM at pH 8.2. Adding 2 or 6 mM of PC:PG 90:10 LUVs resulted in the same $PMMA_{48}$-*b*-$PDMAEMA_{324}$ copolymer's ^{1}D ^{1}H NMR spectrum (data not shown), indicating that the copolymer is already wholly bound in the presence of 2 mM LUVs.

The effect of the pH on the binding of LUVs of PC: PG 90:10 with $PMMA_{48}$-*b*-$PDMAEMA_{324}$ at pH 6.2, 8.2, and 10.0 was studied. The NMR spectra of the copolymer in the absence and presence of 2 mM LUVs of PC:PG 90:1 was acquired (Figure 8). Overall, the peaks corresponding

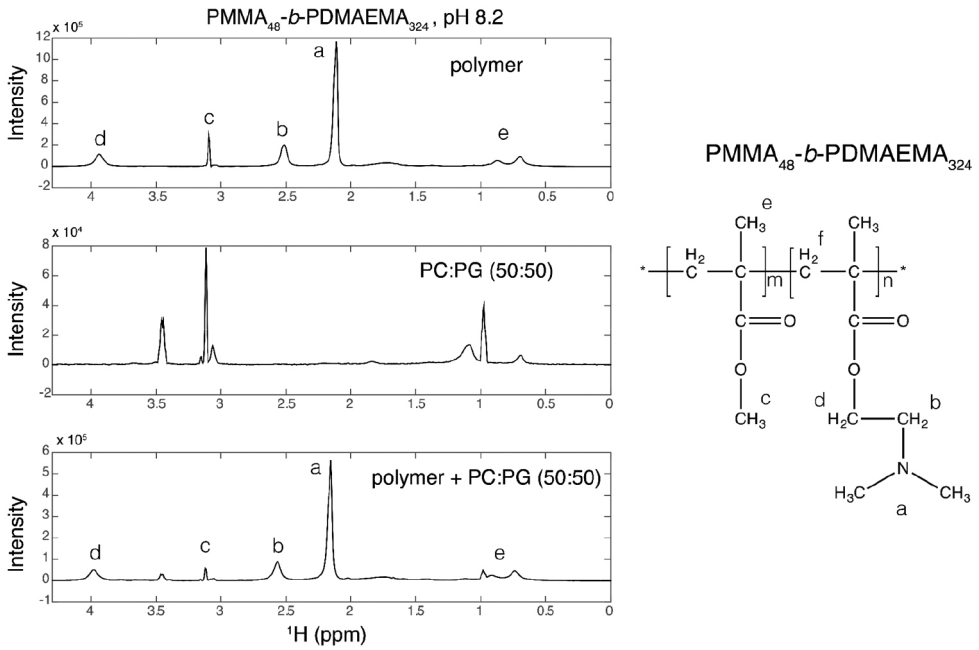

Figure 7. Effect of LUVs of PC:PG 50:50 on the ^{1}H NMR spectrum of 0.1 mM $PMMA_{48}$-*b*-$PDMAEMA_{324}$ in 0.01 M phosphate buffer, pH 8.2. The figures correspond to $PMMA_{48}$-*b*-$PDMAEMA_{324}$ (5.8 mg mL^{-1}) (upper) and PC:PG 50:50, 2 mM (middle). The bottom figure corresponds to the mixture of $PMMA_{48}$-*b*-$PDMAEMA_{324}$ (5.8 mg mL^{-1}) and LUVs of PC:PG 50:50 (2 mM).

to the copolymer's protons were shifted downfield upon the presence of LUVs at lower pH, such as 6.2 and 8.2, showing clear evidence of binding at these two pHs. Interestingly, more significant chemical shifts were observed at pH 6.2 compared to the same experiment performed at pH 8.2. However, a more substantial change in peak intensity

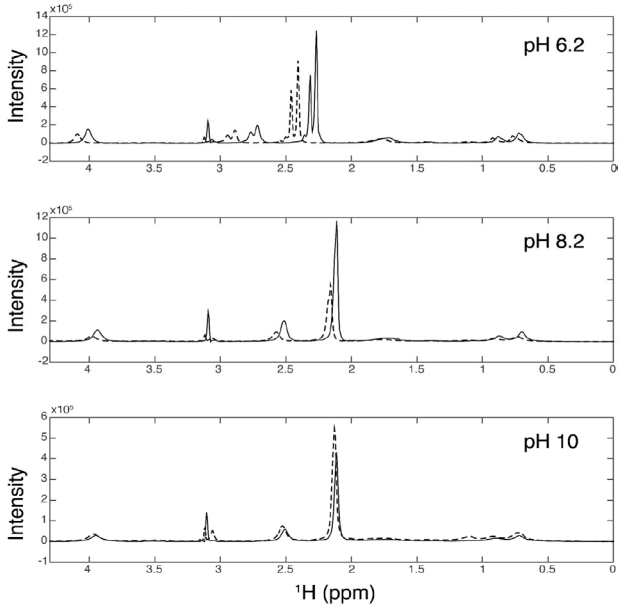

Figure 8. ^{1}H NMR spectra of $PMMA_{48}$-*b*-$PDMAEMA_{324}$ at different pHs: (a) pH 6.2, (b) pH 8.2, and (c) pH 10. $PMMA_{48}$-*b*-$PDMAEMA_{324}$ concentration was 5.8 mg mL^{-1} in all experiments, and the concentration of LUVs of PC:PG 90:10 was 2 mM in lipids. The continuous line corresponds to the copolymer alone, and the dashed line spectrum to the copolymer with the PC:PG LUVs at different pHs, given in the figures.

(broadening) was observed at pH 8.2 than at pH 6.2, revealing a stronger interaction of the copolymer with the LUVs at pH 8.2 compared to pH 6.2. At pH 10.0, the spectrum of the copolymer in the presence and absence of LUVs was very similar, with no significant changes in peak intensities and chemical shifts. Thus, the NMR data suggests that at higher pH values, such as pH 10, weaker interaction is observed compared to lower pH's.

Antimicrobial activity of the polymers

Except for PMMA, all other copolymers evaluated showed antimicrobial activity (Table 2). $PMMA_{50}$ did not cause membrane permeabilization in the CF leak assay, nor any antimicrobial activity was detected.

The methanol used to solubilize the copolymers did not affect the evaluation since bacterial growth was observed in the control using only methanol. The minimum bacterial concentration (MBC) values were the same as the MIC values since bacterial growth was observed after transferring the contents of the microplate well where the bacteria grew to an agar plate. Thus, these copolymers can be considered to have bactericidal activity. The activity was more significant, with lower MIC values, against Gram-positive bacteria than for Gram-negative bacteria.

An increase in the PDMAEMA fraction in the copolymer led to a decrease in the MIC value. This observation is related to the correlation observed in CF

leakage, where a more significant amount of PDMAEMA increases CF leakage, that is, more disturbance in the membrane.

Considering the data dispersion, only $PMMA_{48}$-*b*-$PDMAEMA_{324}$ showed a similar MIC to that of $PDMAEMA_{265}$ homopolymer. Therefore, the PMMA block's presence somehow hindered the polymeric antibacterial effect of the material in that case, suggesting that the PDMAEMA block was the essential feature for antimicrobial activity. To sort out the impact of each block, a specific PDMAEMA content in mass may be calculated, considering the PDMAEMA block contribution to the total molar mass of the polymeric material. $PMMA_{50}$-*b*-$PDMAEMA_{269}$ presents 0.89 in mass fraction (see Table 1) of PDMAEMA; $PMMA_{48}$-*b*-$PDMAEM_{324}$, 0.91 and $PMMA_{94}$-*b*-$PDMAEMA_{88}$, 0.60. Correcting the MIC value for both microorganisms using those factors, they are still within mean ± standard deviation of those for $PDMAEMA_{269}$, so it is not possible to say that the antibacterial activity was improved or decreased by the addition of a PMMA block to PDMAEMA. To better compare the MIC values, the values in mg mL^{-1} (not molarity) were considered here.

However, it must be considered that the composition of the Mueller Hinton broth, used in the determination of MIC, is complex, consisting of several protein extracts that can interact with the polymers. Despite this potential inhibitory factor, these polymers showed significant antimicrobial activity, providing an excellent perspective for their use as antibacterial agents.

The trend of the LUV disruption test (Figure 4) was different from that observed in the MIC experiments. $PMMA_{94}$-*b*-$PDMAEMA_{88}$ was the most effective as a LUV disruptor, mainly if the concentration is considered (not molarity, because this is the one with significantly lower molar mass). The antibacterial activity is more complex than the process of LUV permeabilization, so even though direct membrane interaction must be involved in bacteria inhibition, other phenomena must be in place.

Conclusions

Copolymers of $PMMA_n$-*b*-$PDMAEMA_m$ induced membrane disruption with leakage of the internal PC:PG vesicle content, which was strongly pH-dependent. LUVs-copolymer interaction may lead to vesicle aggregation, depending on the ratio between the copolymer concentration and the PC:PG ratio in the vesicles. We also demonstrated the interaction of polymers with GUVs at different pH's using microscopy.

The pH was essential for the interaction of these copolymers with PC:PG LUVs and GUVs because the positive charge of the polymers is a necessary force that leads to the initial binding to the bilayer of PC:PG vesicles. A hydrophobic region in the copolymer facilitates the interaction with the vesicles. This effect can also be observed at pHs where part of the PDMAEMA moiety is partially uncharged. At pH 6.2, the copolymer is fully charged, and vesicle-polymer interaction was demonstrated (see NMR results, higher chemical shift perturbation observed for peaks from copolymers Figure 8). Chemical shift perturbations and significant intensity decrease are observed at pH 8.2. This latter effect can be explained by the presence of both hydrophobic and positively charged groups in the copolymer, contributing to optimal interaction with PC:PG LUVs and, thus, as observed in the NMR and leakage assays, respectively (Figures 7 and 4). The most significant leakage was observed at pH 8.2 compared to pH 6.2. The optimal balance between hydrophobic and positively charged groups in the copolymer at this pH possibly enhances its interactions with LUVs. The polymer $PMMA_{50}$ alone did not induce LUVs leakage, but it does not mean that it does not bind to the LUVs.

NMR also showed the interaction between the polymers and LUVs. The polymers' PDMAEMA amino groups interact with the PG's charged phosphate groups. The pH increase significantly affects the interaction, and a maximum effect at pH near 8.5, where only part of the amino groups of the copolymers are dissociated. The neutralization of part of

Table 2. MIC of copolymers against *Escherichia coli* (*E.c.*) and *Bacillus subtilis* (*B.s.*)

Copolymer	MIC / μM		MIC / (mg mL^{-1})	
	E.c.	*B.s.*	*E.c.*	*B.s.*
$PMMA_{50}$-*b*- $PDMAEMA_{269}$	12 ± 9	1 ± 0.5	0.5 ± 0.4	0.05 ± 0.02
$PMMA_{48}$-*b*-$PDMAEMA_{324}$	3 ± 1	0.6 ± 0.6	0.2 ± 0.1	0.03 ± 0.03
$PMMA_{94}$-*b*-$PDMAEMA_{88}$	103 ± 34	11 ± 5	2.4 ± 0.8	0.25 ± 0.11
$PDMAEMA_{265}$	3 ± 1	1.0 ± 0.6	0.12 ± 0.05	0.04 ± 0.02
$PMMA_{50}$	nd	nd	nd	nd

nd: antimicrobial activity was not detected until 240 μM (1.2 mg mL^{-1}); MIC: minimum inhibitory concentration; PMMA: poly(methacrylate); PDMAEMA: poly((dimethylamino ethyl) methacrylate).

the amino groups of the copolymer decreases the electrostatic interaction of the polymer with PC:PG LUVs but increases the hydrophobicity of the polymer facilitating the permeation through the bilayer. The complete dissociation of the amino groups, near pH 10, almost eliminates the interaction of the polymers with PC:PG LUVs.

These pH-sensitive $PMMA_n$-*b*-$PDMAEMA_m$ polymers showed significant antimicrobial activity against *E. coli* and *B. subtilis*. The pH dependence observed in the model systems is relevant,[40] since different mammalian organs also present different local pH (an opportunity to target the antimicrobial action) and bacteria are known to modify the acidity of the environment, and adequate polymer surface deposition can provide maximum antimicrobial activity triggered by the pH.

Supplementary Information

Supplementary data are available free of charge at http://jbcs.sbq.org.br as PDF file.

Acknowledgments

The authors thank Analytical Instrumentation Center of the University of São Paulo for NMR instrumentation. FHF thanks the National Council for Scientific and Technological Development, CNPq (grant No. 457733/2014-4), IMC, HC, and FHF thank FAPESP (Proc. 2013/08166-5). IMC thanks CNPq (grant No. 465259/2014-6). IMC and HC thank the Coordination for the Improvement of Higher Education Personnel (CAPES), the National Institute of Science and Technology Complex Fluids (INCT-FCx), and NAP-FCx (Núcleo de Apoio à Pesquisa de Fluidos Complexos da Universidade de São Paulo). G.P.B. Carretero thanks CAPES: INCT -Institutos Nacionais de Ciência e Tecnologia (Proc. 88887.137085/2017-00) and FAPESP (2018/15230-5). GKVS thanks CAPES (proc. no. 23038.004630/2014-35, Projeto Biocomputacional) and CNPq (proc. 457733/2014-4). VVS acknowledges CNPq for his fellowship. We thank Peter Park for his helpful suggestions.

Author Contributions

IMC was responsible for conceptualization; GKS for lead investigation; VVS, AP, MTM, INA, RCFY, CDL, GPBC, RBL, LCO, KAR, RKS for support investigation; LCO, KAR, RKS, HC, FHF, IMC for formal analysis (equal); IMC, FHF for funding acquisition; LCO, RKS, HC, FHF, IMC for writing original draft and writing-review and editing.

References

1. Ghosh, C.; Sarkar, P.; Issa, R.; Haldar, J.; *Trends Microbiol.* **2019**, *27*, 323. [Crossref]
2. Ergene, C.; Yasuhara, K.; Palermo, E. F.; *Polym. Chem.* **2018**, *9*, 2407. [Crossref]
3. Álvarez-Paino, M.; Muñoz-Bonilla, A.; Fernández-García, M.; *Nanomaterials* **2017**, *7*, 48. [Crossref]
4. Carmona-Ribeiro, A.; de Melo Carrasco, L.; *Int. J. Mol. Sci.* **2013**, *14*, 9906. [Crossref]
5. Huan, Y.; Kong, Q.; Mou, H.; Yi, H.; *Front. Microbiol.* **2020**, *11*, 582779. [Crossref]
6. Timofeeva, L.; Kleshcheva, N.; *Appl. Microbiol. Biotechnol.* **2011**, *89*, 475. [Crossref]
7. Bechinger, B.; Gorr, S.-U.; *J. Dent. Res.* **2017**, *96*, 254. [Crossref]
8. Park, P.; Franco, L. R.; Chaimovich, H.; Coutinho, K.; Cuccovia, I. M.; Lima, F. S.; *Sci. Rep.* **2019**, *9*, 8622. [Crossref]
9. Jiao, Y.; Niu, L.; Ma, S.; Li, J.; Tay, F. R.; Chen, J.; *Prog. Polym. Sci.* **2017**, *71*, 53. [Crossref]
10. Jain, A.; Duvuri, L.S.; Farah, S.; Beyth, N.; Domb, A. J.; Khan, W.; *Adv. Health Mater.* **2014**, *3*, 1969. [Crossref]
11. Hu, Y.; Du, Y.; Yang, J.; Kennedy J.; Wang, X.; Wang, L.; *Carbohydr. Polym.* **2007**, *67*, 66. [Crossref]
12. Shima, S.; Matsuoka, H.; Iwamoto, T.; Sakai, H.; *J. Antibiot.* **1984**, *37*, 1449. [Crossref]
13. Ikeda, T.; Hirayama, H.; Yamaguchi, H.; Tazuke, S.; Watanabe, M.; *Antimicrob. Agents Chemother.* **1986**, *30*, 132. [Crossref]
14. Palermo, E. F.; Kuroda, K.; *Biomacromolecules* **2009**, *10*, 1416. [Crossref]
15. Tew, G. N.; Scott, R. W.; Klein, M. L.; DeGrado, W. F.; *Acc. Chem. Res.* **2010**, *43*, 30. [Crossref]
16. Corrigan, N.; Jung, K.; Moad, G.; Hawker, C. J.; Matyjaszewski, K.; Boyer, C.; *Prog. Polym. Sci.* **2020**, *11*, 101311. [Crossref]
17. Monteiro, M. J.; de Brouwer, H.; *Macromolecules* **2001**, *34*, 349. [Crossref]
18. Braunecker, W. A.; Matyjaszewski, K.; *Prog. Polym. Sci*. **2007**, *32*, 93. [Crossref]
19. Wang, B.; Xu, Q.; Ye, Z.; Liu, H.; Lin, Q.; Nan, K.; Li, Y.; Wang, Y.; Qi, L.; Chen, H.; *ACS Appl. Mater. Interfaces* **2016**, *8*, 27207. [Crossref]
20. Rauschenbach, M.; Lawrenson, S. B.; Taresco, V.; Pearce, A. K.; O'Reilly, R. K.; *Macromol. Rapid Commun*. **2020**, *41*, 2000190. [Crossref]
21. Liow, S. S.; Chee, P. L.; Owh, C.; Zhang, K.; Zhou, Y.; Gao, F.; Lakshminarayanan, R.; Loh, X. J.; *Macromol. Biosci*. **2019**, *19*, 1800466. [Crossref]
22. Brilmayer, R.; Kübelbeck, S.; Khali,l A.; Brodrecht, M.; Kunz, U.; Kleebe, H.; Buntkowsky, G.; Baier, G.; Andrieu-Brunsen, A.; *Adv. Mater. Interfaces* **2020**, *7*, 1901914. [Crossref]

23. Laurence, J. S.; Nelson, B. N.; Ye, Q.; Park, J.; Spencer, P.; *Int. J. Polym. Mater. Polym. Biomater.* **2014**, *63*, 361. [Crossref]
24. de Souza, V. V.; Carretero, G. P. B.; Vitale, P. A. M.; Todeschini, I.; Kotani, P. O.; Saraiva, G. K. V.; Guzzo, C. R.; Chaimovich, H.; Florenzano, F. H.; Cuccovia, I. M.; *Polym. Bull.* **2022**, *79*, 785. [Crossref]
25. Maximiano, F. A.; da Silva, M. A.; Daghastanli, K. R. P.; de Araujo, P. S.; Chaimovich H.; Cuccovia, I. M.; *Quim. Nova* **2008**, *31*, 910. [Crossref]
26. Ralston, E.; Hjelmeland, L. M.; Klausner, R. D.; Weinstein, J. N.; Blumenthal, R.; *Biochim. Biophys. Acta, Biomembr.* **1981**, *649*, 133. [Crossref]
27. Manzini, M. C.; Perez, K. R.; Riske, K. A.; Bozelli Jr., J. C.; Santos, T. L.; da Silva, M. A.; Saraiva, G. K. V.; Politi, M. J.; Valente, A. P.; Almeida, F. C. L.; Chaimovich, H.; Rodrigues, M. A.; Bemquerer, M. P.; Schreier, S.; Cuccovia, I. M.; *Biochim. Biophys. Acta, Biomembr.* **2014**, *1838*, 1985. [Crossref]
28. Saraiva, G. K. V.; de Souza, V. V.; de Oliveira, L. C.; Noronha, M. L. C.; Masini, J. C.; Chaimovich, H.; Salinas, R. K.; Florenzano, F. H.; Cuccovia, I. M.; *Colloid Polym. Sci.* **2019**, *297*, 557. [Crossref]
29. Rouser, G.; Fleischer, S.; Yamamoto, A.; *Lipids* **1970**, *5*, 494. [Crossref]
30. Patty, P. J.; Frisken, B. J.; *Biophys. J.* **2003**, *85*, 996. [Crossref]
31. Walde, P.; Ichikawa, S.; *Appl. Sci.* **2021**, *11*, 10345. [Crossref]
32. Weinberger, A.; Tsai, F. C.; Koenderink, G. H.; Schmidt, T. F.; Itri, R.; Meier, W.; Schmatko, T.; Schröder, A.; Marques, C.; *Biophys. J.* **2013**, *105*, 154. [Crossref]
33. Wiegand, I.; Hilpert, K.; Hancock, R. E. W.; *Nat. Protoc.* **2008**, *3*, 163. [Crossref]
34. Andrews, J. M.; *J. Antimicrob. Chemother.* **2001**, *48*, 5. [Crossref]
35. Quina, F. H.; Chaimovich, H.; *J. Phys. Chem.* **1979**, *83*, 1844. [Crossref]
36. Jin, Q.; Kirk, M. F.; *Front. Environ. Sci.* **2018**, 6. [Crossref]
37. Baptista, A. L. F.; Coutinho, P. J. G.; Oliveira, M. E. C. D. R.; Gomes, J. I. N. R.; *J. Liposome Res.* **2003**, *13*, 123. [Crossref]
38. Milo, S.; Acosta, F. B.; Hathaway, H. J.; Wallace, L. A.; Thet, N. T.; Jenkins, A. T. A.; *ACS Sens.* **2018**, *3*, 612. [Crossref]
39. Cruciani, O.; Mannina, L.; Sobolev, A.; Cametti, C.; Segre, A.; *Molecules* **2006**, *11*, 334. [Crossref]
40. Hu, J.; Zhang, G.; Ge, Z.; Liu, S.; *Prog. Polym. Sci.* **2014**, *39*, 1096. [Crossref]

Submitted: February 13, 2023
Published online: May 22, 2023